

ANALYSIS OF THE NATURE AND GROWTH OF ELECTROTHERMAL WAVES

A. H. NELSON and M. G. HAINES

Physics Department, Imperial College, London, S.W.7, England

(Received 1 April 1969)

Abstract—Using a linear theory the dispersion relation of electrothermal waves in a seeded, partially ionized gas is derived. Two modes appear, one of which is always damped, while the other is unstable in certain plasma situations. This is the ionization instability and the growth rate has been calculated as a function of the steady state electron temperature, the angle between the steady state current density and the wave vector, the Hall parameter, and the instability wavelength. The dispersion relation differs from previous dispersion relations in that it is more complete, containing the effects of finite ionization-recombination rates, finite degree of ionization, radiation transfer, electron thermal conduction and the combination of both neutral and coulomb collisions.

The results show that for fixed magnetic field the growth rate has a maximum as a function of electron temperature, falling off at low temperatures due to the effects of finite ionization-recombination rates, and at high temperatures due to the decreasing Hall parameter. However if the Hall parameter is kept constant by increasing the magnetic field the growth rate does not fall off until much higher temperatures where the seed becomes nearly fully ionized. Finally the possibility of stabilizing the waves using the damping effect of radiation transfer is discussed.

1. INTRODUCTION

IN A partially ionized gas, where the electron density (n_e) is in Saha equilibrium at the electron temperature (T_e), perturbations of the electron temperature will lead to large perturbations in the electron density. For a density of ionizable particles (n_s) of 10^{22} $1/m^3$, the Saha equation gives $\partial \log n_e / \partial \log T_e \approx 10$ at $T_e = 2000^\circ\text{K}$.

This means that fluctuations in electron temperature will lead to fluctuations in the electron density which are ten times larger. These fluctuations can substantially alter the plasma parameters, such as conductivity and Hall parameter, and the energy balance in the plasma may be altered in such a way as to either damp or amplify the fluctuations. In addition the fluctuations can in general propagate as a wave.

When the electrons are only weakly coupled thermally to the heavy particles (ions and neutrals) due to the large difference in mass, the heavy particle properties are approximately constant and these propagating fluctuations are called electrothermal waves.

In many plasma situations the waves are unstable and the source of the instability is the enhanced local ohmic heating in the regions of increased electron density. If the perturbations in the energy loss mechanisms (elastic losses to the heavy particles, radiation, convection and conduction) are unable to dissipate this excess heat, the electron temperature will rise leading, by ionization, to a further increase in the electron density and so the wave grows.

Experimental observation of these instabilities has been reported by SHIPUK and PASHKIN (1968), ZUKOSKI and GILPIN (1967) and LOUIS (1968), while KERREBROCK (1964), NEDOSPASOV (1966) and ZETTWOOG (1966) have analysed the waves and given expressions for the growth rates.

One of the reasons that these waves are interesting is their effect on the performance

of MHD generators. The working substance of closed loop MHD generators is usually a noble gas seeded with an alkali metal, and it is desirable to elevate the electron temperature above the rare gas temperature as much as possible to increase the electron density and hence the conductivity. Under these conditions electrothermal waves are possible. However, non-uniformities in the electron density and temperature in the generator will have a damaging effect on the performance. This is because the effective internal impedance is increased and the effective Hall parameter is decreased (ROSA, 1962), leading to a decrease in output and efficiency. It is therefore desirable to stabilize the fluctuations if possible.

In addition to electrothermal waves another type of instability can occur in a partially ionized gas; the so-called magnetosonic instability. In the theory of these waves thermal coupling between the electrons and the heavy particles is assumed to be strong and all species are considered to have a common temperature. The heavy particle properties fluctuate in this wave and basically it is a sound wave which is amplified by $\mathbf{j} \times \mathbf{B}$ forces and ohmic heating. The growth rates of this instability have been calculated (MCCUNE, 1964; HEYWOOD *et al.*, 1967) to be $\sim 10^3$ 1/sec, whereas growth rates for the electrothermal instabilities can be $\sim 10^6$ 1/sec. Hence the electrothermal instability is potentially much more dangerous as far as MHD generators are concerned.

The object of this paper is first of all to derive a complete dispersion relation for small amplitude electrothermal waves, including all the relevant physics of the plasma (radiation, thermal conduction, finite ionization and recombination rates and the variation of all the plasma parameters with electron density and temperature); and secondly to solve the complicated dispersion relation numerically for the growth rate as a function of the steady state plasma parameters. From this analysis it is hoped to find the ranges of plasma parameters (especially electron temperature) for which the waves are stable.

The previous theoretical works on the subject of electrothermal waves have usually made simplifying assumptions such as infinite ionization rates, neglect of radiation, low degree of ionization etc. collision frequency constant with temperature and density, and either neutral collisions dominant or coulomb collisions dominant; although Kerrebrock has a section with finite ionization rates, and Nedaspasov includes a finite degree of ionization. The expressions they derive, however, are still incomplete yet fairly complicated and it is difficult to obtain a clear picture of how the growth rate varies with different plasma situations. It is hoped that plotting graphs of the growth rate against the plasma parameters leads to greater clarity.

It is expected that the effect of finite ionization rates will be to damp the waves at low temperatures. If we look at the equation for change of electron density using the collisional-radiative theory (HINNOV *et al.*, 1962; BATES *et al.*, 1962a, b) for the recombination coefficient and assuming that the equilibrium state is Saha equilibrium at the electron temperature we have

$$\frac{\partial n_e}{\partial t} = A_1 n_e (n_s - n_e) - A_2 n_e^3 \quad (1)$$

where

$$A_2 = 1.1 \times 10^{-20} \times T_e^{-9/2} \frac{m^6}{\text{sec}}$$

and

$$A_1 = \left(\frac{2\pi m_e k T_e}{h^2} \right)^{3/2} \exp \left(- \frac{e V_I}{k T_e} \right) A_2$$

and V_I = ionization potential of the seed.

Supposing that we have a perturbation n_e' in the electron density, we can then find the characteristic time it takes for the equilibrium to be re-established in the absence of destabilising effects. Linearizing with respect to n_e the equation becomes

$$\frac{\partial n_e'}{\partial t} = -n_e' A_2 n_{e0}^2 \left[\frac{2n_s - n_{e0}}{n_s - n_{e0}} \right]$$

(where dashes represent perturbed quantities and zero subscripts represent steady state quantities). Hence for $n_s \gg n_{e0}$ we have

$$\frac{\partial n_e'}{\partial t} = - \frac{n_e'}{\tau_s}$$

where

$$\tau_s = \frac{1}{2n_e^2 A_2}$$

Physically it seems likely that the relaxation rate $1/\tau_s$ is an upper limit to the growth rate of an electrothermal instability. Since $1/\tau_s$ decreases rapidly with electron temperature, this ought to have a significant damping effect on the waves at low temperatures, but a negligible effect at high temperatures.

The results of our calculations show the existence of this damping effect at low temperatures.

The collisional-radiative ionization theory should give a good approximation to the behaviour of the plasma at the electron densities and temperatures considered. However recent papers (SHAW *et al.*, 1966; SURDO, 1967) have thrown doubt on the assumption that the equilibrium state is in Saha equilibrium at the electron temperature. They indicate that the electron density in the steady state may be reduced below the Saha level. With no other analytic expression for the equilibrium state available, Saha's equation has been used for the zero-order equilibrium. The effect of a reduced electron density at equilibrium is equivalent to reducing the ionization rate, and hence will tend to stabilize the electrothermal waves. Using Saha equilibrium for the steady state therefore gives an upper limit for the growth rate.

Since the instabilities are dependent on the partially ionized nature of the caesium seed it is expected that when the seed becomes almost fully ionized the instabilities will die away. The important parameter here is $\partial \log n_e / \partial \log T_e$ which from Fig. 1 ~ 10 at about 2000°K for caesium and decreases with temperature. Unfortunately $\partial \log n_e / \partial \log T_e$ does not decrease to below 1 until $T_{e0} > 5000^\circ\text{K}$, and because of this the damping effect of a finite degree of ionization does not appear until this temperature.

In fact however we find that for fixed magnetic field ($\sim 1 \rightarrow 10$ tesla) the growth rate reaches a maximum and falls off with increasing temperature well below 5000°K. This is due to the value of Hall parameter (β_0) decreasing below a critical value of the order of 1, which causes the ohmic heating to fall below the energy losses in the wave.

The radiation term used in the calculations is that derived by LUTZ (1967). The basic assumption is that the first doublet excitation level of the caesium seed atoms, which dominates the radiation energy losses, is populated at L.T.E. with respect to the electron gas; i.e. we assume that the level is populated by inelastic collisions with electrons, and radiative excitations and de-excitations play only a small role. Due to the large self absorption which increases the effective lifetime of an excited state, and the high electron densities this is a good approximation in our plasmas.

Although the photons in the plasma play a small role in determining the population densities of the excited levels they play an important role in damping a sinusoidal instability by transferring energy from the peaks to the troughs. By increasing the radiation damping in the wave it is theoretically possible that under a wide range of conditions stability can be achieved.

2. BASIC EQUATIONS

Assumptions

We make the following assumptions about the state of the four component (electrons, seed ions, seed atoms and neutral buffer atoms) plasma:—

(1) The electrons have a Maxwellian distribution in velocity space.

(2) The electron number density n_e and the ion number density n_i are equal.

This is not strictly true of course since space charge electric fields exist as a result of the fluctuations. However the difference in electron and ion number densities required to produce these fields is very small compared to the fluctuation amplitudes of the two densities. This can be seen as follows. Poisson's equation for the perturbed state is

$$\nabla \cdot \mathbf{E}' \sim \frac{2\pi\mathbf{E}'}{\lambda} \sim \frac{(n_i' - n_e')e}{\epsilon_0}$$

where λ = fluctuation wavelength, and the linearized Ohm's law equations (2) and (7) gives $E'/E_0 \sim n_e'/n_{e0}$.

Hence $(n_i' - n_e') \sim 2\pi\epsilon_0 E_0 n_e' / e\lambda n_{e0}$ and for $\lambda = 10^{-2}$ m, $E_0 = 10^4$ V/m, and $n_{e0} = 3 \times 10^{20}$ m⁻³ say, we have $n_i' - n_e' \sim 10^{-6} n_e'$.

(3) The heavy particles have the same temperature, i.e.

$$T_i = T_a = T_n = T, \text{ but } T_e \neq T.$$

The equality of the ion, seed and neutral temperatures follows from their approximately equal mass. The thermal coupling between them is strong, while the much lighter electrons are partially uncoupled thermally from the other components.

(4) The heavy particles have the same centre of mass velocity, i.e. $\mathbf{v}_i = \mathbf{v}_a = \mathbf{v}_n = \mathbf{v}$, i.e. no ion or seed slip.

(5) T , \mathbf{v} , n_n and n_s are all constant in space and time.

We assume therefore that the steady state is 'uniform' i.e. that $L \gg \lambda$ where L = characteristic length over which the steady state variables change. Furthermore we assume that the heavy particles do not participate in the waves. This is equivalent to assuming that the characteristic times of the waves (period and growth time) are so small that the heavy particles do not have time to move; and also that the thermal capacity of the heavy particles is such that the fluctuations in T are negligible.

(6) The magnetic field, $\mathbf{B} = (0, 0, B)$, is constant in space and time, i.e. zero

Reynold's number. This is a good approximation for the characteristic conductivities, wavelengths and velocities in MHD generators. To compare $B^* \equiv B'/B_0$ (quantities with the superscript*, equal to the ratio of the perturbed to the steady state value, we call the fluctuation) with $n_e^* \equiv n_e'/n_{e0}$ for instance, we have $\nabla \times B'/\mu_0 \sim 2\pi B'/\mu_0 \lambda \sim j'$. From the linearization of Ohm's Law we have $j' \sim j_0 n_e^* \sim \sigma v B n_e^*$ and hence $2\pi B^* \sim (\sigma v \mu_0 \lambda) n_e^*$. For $\sigma = 1$ mho/m, $v = 10^3$ m/sec and $\lambda = 10^{-2}$ m we have $B^* \sim 10^{-6} n_e^*$.

Under these approximations the plasma state is described by three electron equations (density, momentum and energy), and two field equations.

In the heavy particle frame of reference, i.e. $\mathbf{v} = 0$, these are given below in rationalised M.K.S. units.

Electron density

This is equation (1) given above.

Electron momentum (Ohm's Law)

The two components of Ohm's Law perpendicular to the magnetic field are:—

$$\left. \begin{aligned} j_x &= \frac{\sigma}{1 + \beta^2} (F_x - \beta F_y) \\ j_y &= \frac{\sigma}{1 + \beta^2} (\beta F_x + F_y) \end{aligned} \right\} \text{— (we assume } E_z, \text{ and } \partial/\partial z \equiv 0) \quad (2)$$

where $\mathbf{F} = \mathbf{E} + \frac{\nabla p_e}{n_e e}$,

$$p_e = n_e k T_e,$$

$$\sigma = \frac{n_e e^2}{m_e \nu},$$

$$\beta = \frac{Be}{m_e \nu}.$$

The total collision frequency ν of the electrons is the sum of the Coulomb collision frequency ν_{coul} and the binary collision frequency ν_B with ions and neutrals respectively.

i.e. $\nu = \nu_{\text{coul}} + \nu_B$

where

$$\nu_{\text{coul}} = \frac{n_e}{6} (\pi k T_e)^{-3/2} \frac{e^4}{\epsilon_0^2 \sqrt{2m_e}} \log \Lambda$$

$$\Lambda = \frac{12\pi}{e^3} \left(\frac{\epsilon_0^3 k^3 T_e^3}{n_e} \right)^{1/2}$$

$$\nu_B = n_n \left(\frac{3 k T_e}{\pi m_e} \right)^{1/2} q_{en}$$

and (OVCHARENKO, 1969)

$$q_{en} = [6.0 + 5.5 \times 10^{-3}(T_e - 2000)] \times 10^{-21} m^2.$$

Electron energy equation

$$\frac{\partial U_e}{\partial t} - \nabla \cdot \left(\frac{U_e \mathbf{j}}{n_e e} \right) - p_e \nabla \cdot \left(\frac{\mathbf{j}}{n_e e} \right) = \frac{\mathbf{j}^2}{\sigma} - 3n_e k(T_e - T) \left[v_{\text{coul}} \frac{m_e}{m_s} + v_B \frac{m_e}{m_n} \right] - \frac{\partial n_e}{\partial t} e V_I - R + \nabla(\kappa \nabla T_e) \quad (3)$$

where the internal energy density is given by

$$U_e = 3/2 n_e k T_e$$

and the thermal conductivity by

$$\kappa = \frac{n_e k^2 T_e}{m_e \nu} \frac{5/2}{1 + \beta^2}.$$

The radiation in the plasma is dominated by the lowest order caesium doublet ($6^2S_{1/2} - 6^2P_{1/2}$, $6^2S_{1/2} - 6^2P_{3/2}$). Since the absorption length of this resonance radiation is small compared to the dimensions of most plasmas under consideration the radiation is largely trapped. Using the expression derived by LUTZ (1967) for an infinite plasma we have

$$R(y) = \sum_i \left\{ 2\pi B_i(y) \Delta v_i m_{pi}^{1/2} \times \int_0^{m_{pi}} m_v^{-1/2} \left(1 + \frac{m_v}{2m_{pi}} \right) dm_v - \pi \Delta v_i m_{pi}^{1/2} \times \int_0^{m_{pi}} m_v^{1/2} \left(1 + \frac{m_v}{2m_{pi}} \right) dm_v \times \int_y^\infty \frac{dz}{z} \times \left[\int_y^\infty B_i(t) \exp(-m_v z(t-y)) dt + \int_{-\infty}^y B_i(t) \exp(-m_v z(y-t)) dt \right] \right\}.$$

The summation is over the two resonance lines, and

$$B_i(y) = \frac{2h\nu_i^3}{c^2} \frac{1}{\exp\left(\frac{h\nu_i}{kT_e(y)}\right) - 1}$$

$$m_{pi} = \frac{n_{aG}}{4\pi^2} \lambda_i^2 \frac{g_{Ei}}{g_0} \frac{1}{\Delta v_i \tau_i}$$

$$\Delta v_i = \rho_i^2 n_n \sqrt{\left(\frac{8kT}{\pi m_n}\right)}.$$

The first term represents emission from the volume element and the second two represent absorption from the rest of the plasma. It is assumed that the population density n_{ai} of each excited state is dominated by collisional excitation and de-excitation so that

$$n_{ai} = n_{aG} \exp(-h\nu_i/kT_e) \times \frac{g_{Ei}}{g_0}$$

and

$$n_{aG} + \sum_i n_{ai} = n_a$$

$$\text{i.e. } n_{aG} = n_a / \left(1 + \sum_i \exp\left(-\frac{h\nu_i}{kT_e}\right) \right).$$

The dominant absorption line broadening mechanism is Van der Waals broadening by the neutral atoms. The values of λ_i , g_{Ei} , and τ_i used are those given by CORLISS and OZMAN (1962), and ρ_i is calculated from a formula given by GRIEM (1964).

Charge conservation equation

$$\nabla \cdot \mathbf{j} = 0 \tag{4}$$

using assumption (1).

Faraday's Law

$$\nabla \times \mathbf{E} = 0 \tag{5}$$

using assumption (6).

This is a set of 6 equations in the 6 unknowns E_x, E_y, j_x, j_y, n_e and T_e . Boundaries will normally give some sort of condition on \mathbf{E} and \mathbf{j} ; for instance a circuit equation.

Here we make the assumption that the plasma is infinite and plane wave solutions are applicable to the first order perturbation of the above set of equations. This enables us to eliminate \mathbf{E} and one component of \mathbf{j} from the equations while reducing their number to three.

3. ZERO ORDER EQUATIONS

The steady state of the plasma is assumed to be uniform and the first three equations reduce to:—

$$\frac{n_{e0}^2}{n_s - n_{e0}} = \frac{A_1}{A_2}$$

i.e. we assume that Saha equilibrium holds in the steady state electron momentum (Ohm's Law):

$$j_{x0} = \frac{\sigma_0}{1 + \beta_0^2} (E_{x0} - \beta_0 E_{y0})$$

$$j_{y0} = \frac{\sigma_0}{1 + \beta_0^2} (\beta_0 E_{x0} + E_{y0})$$

electron energy:

$$\frac{j_0^2}{\sigma_0} = 3n_{e0}k(T_{e0} - T) \left[\nu_{\text{coul0}} \frac{m_e}{m_s} + \nu_{BO} \frac{m_e}{m_n} \right]$$

i.e. the ohmic heating is transferred from the electrons to the heavy particles. The radiation transfer term is zero in the steady state (evaluation of the integrals in R for a uniform plasma easily demonstrates this) since each part of the plasma is absorbing as much as it emits. For a finite plasma, however, the limits of the integral would be different and R would be non zero. Physically this means we have radiation escaping from a finite plasma; however, for the resonance radiation the absorption length (typically $\sim 10^{-5}m$) is very much smaller than the dimensions of most MHD laboratory plasmas and the radiation escape is small compared to the elastic loss to the heavy particles. We assume therefore that the steady state of our infinite plasma model is a good approximation to that in a finite plasma.

Note that strictly speaking our assumptions of a uniform steady state and ohmic heating of the heavy particles through the equipartition term are incompatible. The heavy particles must get rid of the energy either by convection or conduction,

or both. The implicit assumption therefore is that the velocity of convection or the thermal conductivity is large enough for the condition $L \gg \lambda$ to hold, and also the heavy particle background should remain in a uniform state during the times of interest of the electrothermal wave.

4. FIRST ORDER EQUATIONS

Equation (1) linearizes in a straightforward manner to the form

$$\frac{\partial n_e^*}{\partial t} = a_0 T_e^* + b_0 n_e^* \quad (6)$$

where

$$b_0 = b T_{e0}^{-9/2} n_{e0}^{-2} \frac{(n_{e0} - 2n_s)}{n_s - n_{e0}} \quad b = 1.1 \times 10^{-20},$$

and

$$a_0 = b T_{e0}^{-9/2} n_{e0}^{-2} \left(3/2 + \frac{eV_I}{kT_{e0}} \right).$$

The linearization of equation (2) is more complicated, and involves equations (4) and (5). Assuming plane wave solutions with the wave vector defining the y -direction (i.e. all perturbed quantities are proportional to $\exp(i\omega t - iKy)$), we have

$$\partial/\partial x, \partial/\partial z \equiv 0$$

hence from equation (4) we have

$$\frac{\partial j_y'}{\partial y} = 0 \text{ i.e. } j_y' = 0$$

and therefore $\mathbf{j}' = (j_x', 0, 0)$. Similarly equation (5) gives $\partial E_x'/\partial y = 0$ i.e. $E_x' = 0$ and therefore $F_x' = 0$. Now we can linearise equation (2) to obtain F_y' in terms of σ' and β' , and substitute for F_y' in j_x' . Thus we arrive at

$$j_x' = \sigma' F_{x0} - \frac{\beta' \sigma_0}{1 + \beta_0^2} [\beta_0 F_{x0} + F_{y0}].$$

Using $\sigma(T_e, n_e)$ and $\beta(T_e, n_e)$ as defined above, we further reduce the Ohm's Law to

$$\begin{aligned} \frac{j_x'}{j_0} = & -T_e^* \left\{ \frac{3}{2} \sin \alpha \left[\frac{\nu_{\text{coul}0}}{\nu_0} \left(\frac{1}{\log \Lambda_0} - 2 \right) + 1 \right] \right\} + n_e^* \left\{ \left[1 - \frac{\nu_{\text{coul}0}}{\nu_0} \right. \right. \\ & \left. \left. \times \left(1 - \frac{1}{2 \log \Lambda_0} \right) \right] [\sin \alpha + \beta_0 \cos \alpha] + \frac{\nu_{\text{coul}0}}{\nu_0} \left(1 - \frac{1}{2 \log \Lambda_0} \right) \beta_0 \sin \alpha \right\} \quad (7) \end{aligned}$$

where

$$\alpha = \sin^{-1} \left(\frac{(\mathbf{j}_0 \times \mathbf{K}) \cdot \mathbf{B}}{j_0 K B} \right).$$

Linearising the energy equation completes the first order set of three equations in n_e' , T_e' and j_x' . Using equation (7) we can eliminate j_x' from the energy equation which becomes,

$$c_0 \frac{\partial n_e^*}{\partial t} + h_0 \frac{\partial T_e^*}{\partial t} = d_0 n_e^* + f_0 T_e^* \quad (8)$$

where

$$c_0 = (3/2kT_{e0} + eV_I)n_{e0}$$

$$h_0 = 3/2n_{e0}kT_{e0}$$

$$f_0 = -i \frac{3/2kT_{e0}Kj_0 \cos \alpha}{e}$$

$$+ \frac{j_0^2}{\sigma_0} \left\{ 3 \left[\frac{\nu_{\text{coul}0}}{\nu_0} \left(\frac{1}{\log \Lambda_0} - 2 \right) + 1 \right] \left[\frac{1}{2} - \sin^2 \alpha \right] - 3 \left[1 + \left(\frac{3}{\log \Lambda_0} - 2 \right) \frac{\xi_{\text{coul}0}}{\xi_0} \right] \right. \\ \left. - \frac{2T_{e0}}{T - T_{e0}} \right\} + \sum_i 3\pi \left(\frac{h\nu_i}{kT_{e0}} \right)^2 \frac{kT_{e0}}{\lambda_i^2} (m_{0i}K)^{1/2} \Delta\nu_i \exp \left(- \frac{h\nu_i}{kT_{e0}} \right) + \kappa K^2$$

and

$$d_0 = \frac{ikT_{e0}Kj_0 \cos \alpha}{e} + \frac{2j_0^2}{\sigma_0} \left\{ \sin \alpha \left[\left(1 - \frac{\nu_{\text{coul}0}}{\nu_0} \right) \sin \alpha + \beta_0 \cos \alpha \right] \right. \\ \left. - 1 + \frac{1}{2} \left[1 - \frac{1}{2 \log \Lambda_0} \right] \left[\frac{\nu_{\text{coul}0}}{\nu_0} - \frac{\xi_{\text{coul}0}}{\xi_0} \right] \right\}$$

where $\xi_{\text{coul}0}$ = energy loss due to elastic collisions with the ions and ξ_0 = energy loss due to elastic collisions with all the heavy particles.

Here we have substituted $-iK$ for $\partial/\partial y$. Substituting $i\omega$ for $\partial/\partial t$ in (6) and (8) we get two equations of the form

$$\begin{pmatrix} i\omega - b_0 & -a_0 \\ i\omega c_0 - d_0 & i\omega h_0 - f_0 \end{pmatrix} \cdot \begin{pmatrix} n_e^* \\ T_e^* \end{pmatrix} = 0.$$

Hence we get a dispersion relation for the electrothermal waves of the form

$$\det \begin{pmatrix} i\omega - b_0 & -a_0 \\ i\omega c_0 - d_0 & i\omega h_0 - f_0 \end{pmatrix} = 0.$$

This gives us a quadratic in ω with coefficients which are complicated functions of T_{e0} , α , β_0 and K . We have solved this quadratic numerically and have plotted the frequencies and growth rates of the electrothermal waves as a function of these four parameters.

5. RESULTS

(a) Procedure of calculations

The dispersion relation has been solved numerically on the IBM 7094 at Imperial College. In most of the calculations the plasma considered was an argon gas seeded with caesium (the results for this mixture are shown in Figs. 1-17); however, some calculations were also carried out for argon and potassium, helium and potassium, and helium and caesium (results shown in Fig. 18). In all cases the neutral gas has a number density of 10^{25} particles/m³ and the seed fraction is 0.001.

The calculations were carried out with the heavy particle temperature (T) usually fixed at 1500°K and the variations of T_{e0} and B were made to correspond as closely as possible to experimentally realisable situations. For instance T_{e0} was varied for fixed B (α and K also fixed); this corresponds to increasing the internal Ohmic

dissipation in an MHD generator by decreasing the external load. Of course in an experiment this would also cause T to rise slightly, the magnitude of the rise depending on the energy loss mechanisms for the heavy gas. Assuming the consequent rise in T to be small its effect on the growth rate, g , will be small (since g is roughly proportional to the Ohmic heating, j_0^2/σ_0 , which is proportional to $(T_{e0} - T)$); and even if the rise is not small it will not qualitatively affect the way in which g varies with T_{e0} (i.e. the maximum of d as a function of T_{e0} and the stability at high values of T_{e0} will still be present).

T_{e0} was also varied by varying T keeping all other parameters constant including the Ohmic heating.

These two methods of varying T_{e0} have B constant, and for completeness another method of varying T_{e0} was tried. This consists of keeping the external load and T constant but varying the amount of magnetically induced elevation of T_{e0} by varying B . In this case a load factor 0.75 and a gas velocity relative to the magnetic field of 10^3 m/sec were used.

As previously stated, the variation of g with T_{e0} turns out to be qualitatively the same in the first two cases, giving a maximum of g with respect to T_{e0} at 2500°K ; however in the third case g increases with T_{e0} through 2500 and does not start to decrease until T_{e0} is approximately 5000°K .

(b) Wave modes

Since the dispersion relation is a quadratic its solution gives two independent modes for electrothermal waves. Essentially they are a high frequency mode, which is always severely damped, and a low frequency mode which is unstable under certain conditions (see Figs. 1 and 4). In the graphs and in the rest of this paper the high and low frequency modes are referred to as the fast thermal mode and the ionization mode respectively).

If we define the parameters ρ and θ by

$$\rho \exp(+i\theta) = n_e^*/T_e^*.$$

We can see from Fig. 2 that at $T_{e0} = 2500^\circ\text{K}$, $\rho \ll 1$ for the fast thermal mode, while $\rho \sim 10$ for the ionization mode; also from Fig. 3 we see that $\theta \approx \pi$ for the fast thermal mode and $\theta \approx 0$ for the ionization mode. At temperatures lower than 2500°K Fig. 7 shows that θ for the ionization mode is $\approx -\pi$ over a range of values of α where the mode is damped (see Fig. 5). This is due to the finite ionization-recombination rates being a limiting factor at these temperatures, and we will discuss this in more detail in the next section.

For both modes the values of all wave parameters for α and $\alpha + \pi$ are identical, except for the phase velocity and θ , which both change sign. That is, given an orientation of the wave front defined by α , the waves travel in one direction only. For this reason quantities plotted as a function of α are plotted in the range $|\alpha| < \pi/2$ only.

At temperatures below 4650°K the fast thermal and the ionization modes travel in opposite directions, the former has a positive phase velocity for $|\alpha| > \pi/2$ and the latter has a positive phase velocity for $|\alpha| < \pi/2$. That is the fast thermal mode travels in the same sense as the electrons while the ionization mode travels in the opposite sense. However, above 4650°K the phase velocity of the ionization mode reverses (see Fig. 16); the physical reason for this will be explained in Section 5(g).

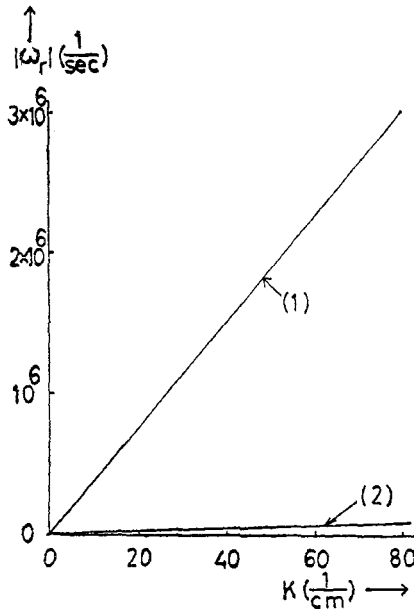


FIG. 1.—Graph of the modulus of the real part of ω vs. wave number. (1) Fast thermal mode; (2) Ionization mode. For both curves:— $T_{e0} = 2500^\circ\text{K}$, $T = 1500^\circ\text{K}$, $\alpha = \pi/4$, $B = 5.0$ tesla.

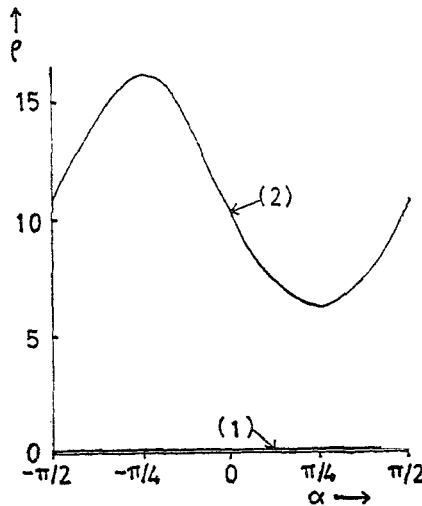


FIG. 2.—Graph of $\text{mod}(n_e^*/T_e^*)$ vs. α (1) Fast thermal mode; (2) Ionization mode. For both curves:— $T_{e0} = 2500^\circ\text{K}$, $T = 1500^\circ\text{K}$, $B = 5.0$ tesla, $\lambda = 1$ cm.

(c) Dependence of the instability on α

The parameters g , ρ , θ and ω_r/K for the ionization mode are plotted as functions of α in the interval $-\pi/2 \rightarrow \pi/2$ for various values of T_{e0} in Figs. 5, 6, 7 and 8 respectively. These curves have constant magnetic field (5 tesla) and it can be seen from Fig. 5 that for low temperatures ($\leq 3000^\circ\text{K}$) there is growth in a range of angles centred about $\alpha \approx \pi/4$. This α -dependence of g is in sharp contrast to that given by KERREBROCK (1964). He predicted that if $\alpha = \pi + \epsilon$ then the growth rate tends to $+\infty$ as $\epsilon \rightarrow 0$ through $+$ ve values, and it tends to $-\infty$ as $\epsilon \rightarrow 0$ through $-$ ve values.

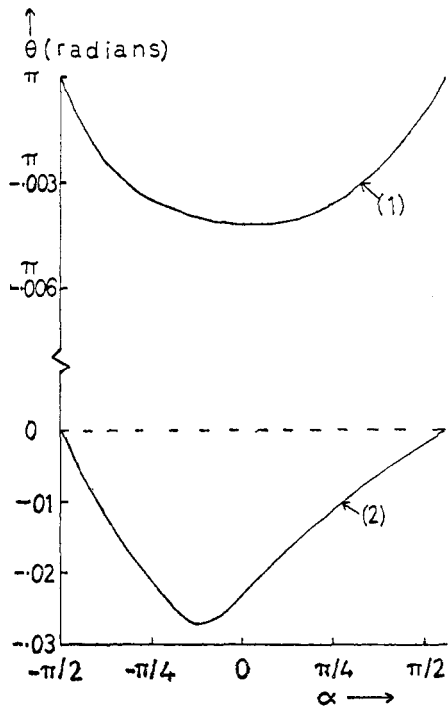


FIG. 3.—Graph of $\arg(n_e^*/T_e^*)$ vs. α . (1) Fast thermal mode; (2) ionization mode. For both curves:— $T_{e0} = 2500^\circ\text{K}$, $T = 1500^\circ\text{K}$, $B = 5.0$ tesla, $\lambda = 1$ cm. (Note θ scale.)

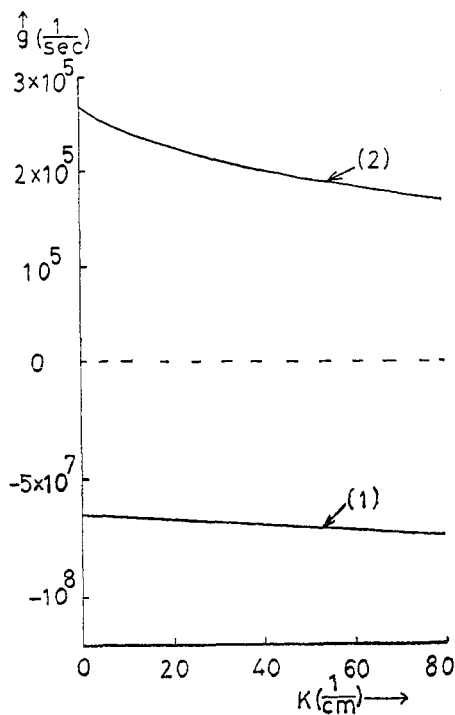


FIG. 4.—Graph of growth rate vs. wave number. (1) Fast thermal mode (2) ionization mode. For both curves:— $T_{e0} = 2500^\circ\text{K}$, $T = 1500^\circ\text{K}$, $\alpha = \pi/4$, $B = 5.0$ tesla. (Note difference in scale above and below the zero axis.)

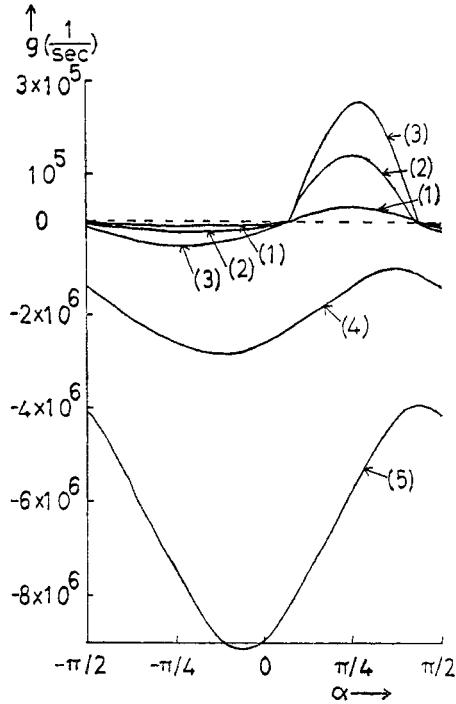


FIG. 5.—Graph of growth rate vs. α (ionization mode). (1) $T_{e0} = 2000^\circ\text{K}$; (2) $T_{e0} = 2250^\circ\text{K}$; (3) $T_{e0} = 2500^\circ\text{K}$; (4) $T_{e0} = 4000^\circ\text{K}$; (5) $T_{e0} = 5500^\circ\text{K}$. For all curves:— $T = 1500^\circ\text{K}$, $\lambda = 1$ cm $B = 5.0$ tesla (note different scale above and below zero axis).

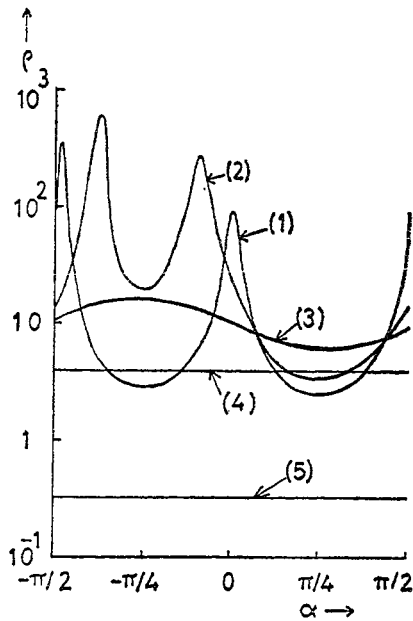


FIG. 6.—Graph of $\text{mod}(n_e^*/T_e^*)$ vs. α (ionization mode). (1) $T_{e0} = 2000^\circ\text{K}$; (2) $T_{e0} = 2250^\circ\text{K}$; (3) $T_{e0} = 2500^\circ\text{K}$; (4) $T_{e0} = 4000^\circ\text{K}$; (5) $T_{e0} = 5500^\circ\text{K}$. For all curves:— $T = 1500^\circ\text{K}$, $\lambda = 1$ cm, $B = 5.0$ tesla.

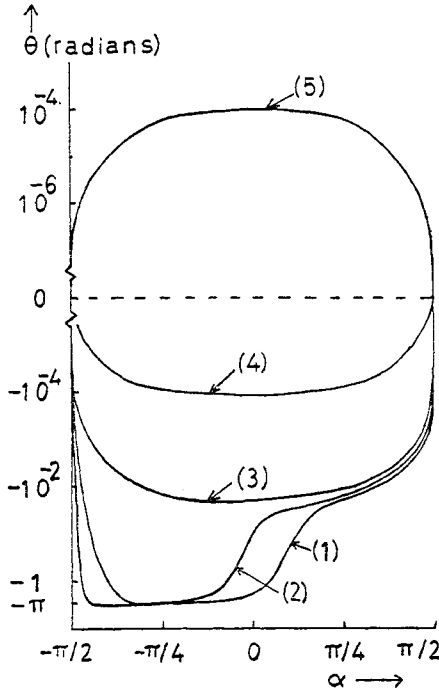


FIG. 7.—Graph of $\arg(n_e^*/T_e^*)$ vs. α (ionization mode). (1) $T_{e0} = 2000^\circ\text{K}$; (2) $T_{e0} = 2250^\circ\text{K}$; (3) $T_{e0} = 2500^\circ\text{K}$; (4) $T_{e0} = 4000^\circ\text{K}$; (5) $T_{e0} = 5500^\circ\text{K}$. For all curves:— $T = 1500^\circ\text{K}$, $\lambda = 1$ cm, $B = 5.0$ tesla.

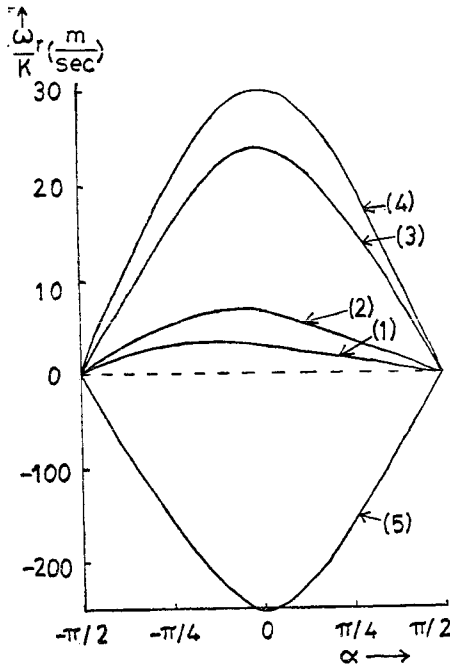


FIG. 8.—Graph of phase velocity (ω_p/K) vs. α (ionization mode). (1) $T_{e0} = 2000^\circ\text{K}$; (2) $T_{e0} = 2250^\circ\text{K}$; (3) $T_{e0} = 2500^\circ\text{K}$; (4) $T_{e0} = 4000^\circ\text{K}$; (5) $T_{e0} = 5500^\circ\text{K}$. For all curves:— $T = 1500^\circ\text{K}$, $\lambda = 1$ cm, $B = 5.0$ tesla. (Note different scale above and below zero axis.)

We think that Kerrebrock's α -dependence is due to an error in his equation (40) where the $(K_y/K)^2$ factor should be $(K_x/K)^2$.

The α -dependence given here is in agreement with a remark by ZETTWOOG (1966) and also with the experimental results of SHIPUK and PASHKIN (1968) and ZUKOSKI and GILPIN (1967).

From Fig. 6 we see that ρ is not a constant with α as it should be if n_e^* and T_e^* were related to each other through the Saha equilibrium equation. Above 2500°K the approximation becomes a good one, but below 2500°K it is not. At 2500°K the value of $\partial \log n_{e0}/\partial \log T_{e0}$ from the Saha equation is approximately 10.5 and we see that ρ equals this value only at $g = 0$. This we would expect since the period of the ionization mode is $\sim 10^{-4}$ secs and the Saha relaxation time is much less than this for $T_{e0} = 2500^\circ\text{K}$. However, when the wave is growing the growth rate is of the order of the Saha relaxation time and the rate of change of the electron density perturbation is limited by the finite ionization and hence the rise in T_e^* gets ahead of the rise in n_e^* making ρ fall below $\partial \log n_{e0}/\partial \log T_{e0}$. Similarly, when the wave is damped the rate of decrease of n_e^* is limited by the finite recombination rate and the fall in T_e^* gets ahead of the fall in n_e^* and ρ rises above $\partial \log n_{e0}/\partial \log T_{e0}$. At lower temperatures the rise and fall of ρ above and below $\partial \log n_{e0}/\partial \log T_{e0}$ is increased because of decreasing ionization and recombination rates, but in the stable range of α a new effect appears. The ionization mode becomes similar to the fast thermal mode in that θ falls to $-\pi$, and the effect of this is to take a large 'bite' out of the rise in ρ leaving two spikes on the edge of the stable range. Figure 7 clearly shows that as the temperature rises the range of α over which $\theta = -\pi$ decreases, the size of the 'bite' decreases and the spikes converge.

From Fig. 8 we see that the phase speed $|\omega_r/K|$ maximises at $\alpha \approx 0$ except at lower temperatures, and at all temperatures $\omega_r/K = 0$ at $\alpha = \pm\pi/2$.

(d) Dependence of the instability on β

The dependence of the growth rate on β_0 is now well known from experimental observations (SHIPUK *et al.*, 1968; ZUKOSKI *et al.*, 1967). The results derived here confirm that the growth rate increases with increasing β_0 and that below a value of $\beta_0 \sim 1$ it is negative (see Fig. 9); also the temperature dependence of the value of β_0 at which the instability starts ($\beta_{0\text{CRIT}}$), shown in Fig. 10 is similar to that previously reported (ANGROLOV *et al.*, 1968; SHIPUK *et al.*, 1968).

The range of α over which we have instability ($\Delta\alpha$) is plotted in Fig. 11 as a function of β_0 at $T_{e0} = 2500^\circ\text{K}$. $\Delta\alpha$ increases with increasing β_0 and could explain why in some experiments (SHIPUK *et al.*, 1968) the initially plane wave instability breaks down into random turbulence as β_0 is increased. This could be due to two or more Fourier components of the initial disturbance oriented in different directions being successively de-stabilized by the increasing range $\Delta\alpha$; i.e. first one component is destabilized giving plane wave fluctuations and then $\Delta\alpha$ increases to include the other(s) giving, along with the first one, apparently random fluctuations.

(e) The growth rate as a function of T_{e0}

The growth rate as a function of the steady state electron temperature is shown in Fig. 12 curve 1 for $T = 1500^\circ\text{K}$, $B = 5.0$ tesla, $\lambda = 1$ cm and $\alpha \approx \pi/4$.

The growth rate shows a maximum with electron temperature at $T_{e0} \approx 2500^\circ\text{K}$

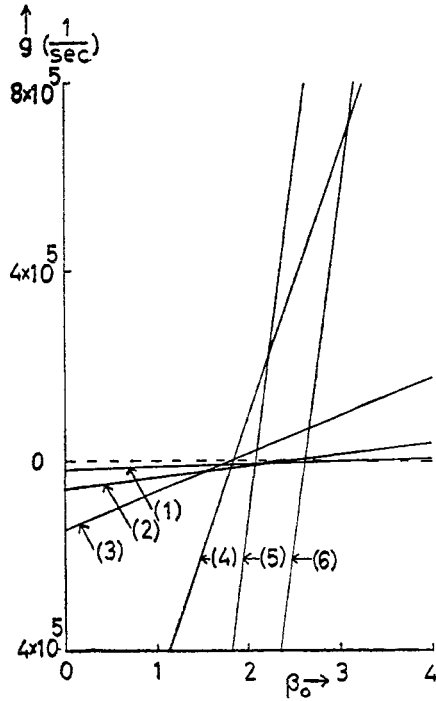


FIG. 9.—Graph of growth rate vs. Hall parameter (ionization mode). (1) $T_{e0} = 2000^\circ\text{K}$; (2) $T_{e0} = 2250^\circ\text{K}$; (3) $T_{e0} = 2500^\circ\text{K}$; (4) $T_{e0} = 3500^\circ\text{K}$; (5) $T_{e0} = 4500^\circ\text{K}$; (6) $T_{e0} = 5000^\circ\text{K}$. For all curves $T = 1500^\circ\text{K}$, $\lambda = 1 \text{ cm}$, $\alpha = \pi/4$.

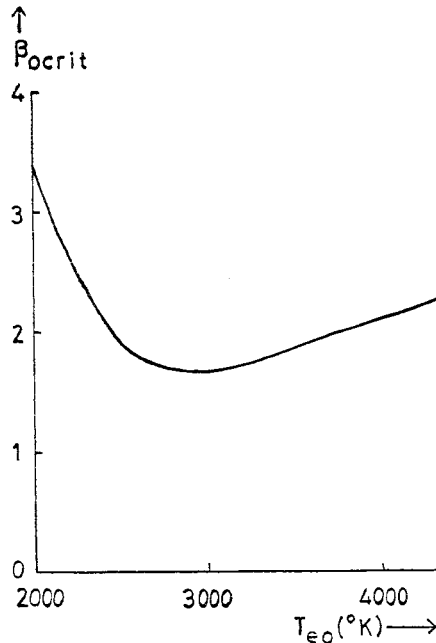


FIG. 10.—Graph of critical Hall parameter for stability vs. electron temperature (ionization mode). $T = 1500^\circ\text{K}$, $\lambda = 1 \text{ cm}$, $\alpha = \pi/4$.

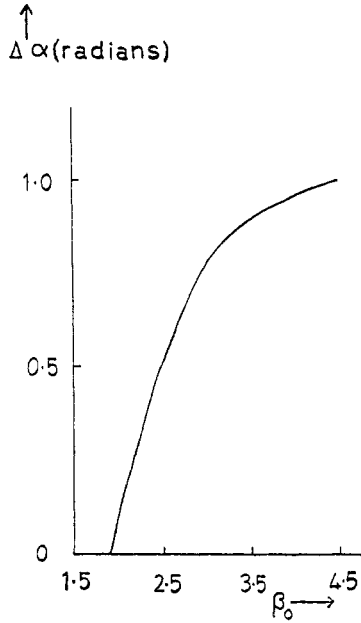


FIG. 11.—Graph of range of angles for instability vs. Hall parameter (ionization mode).
 $T_{e0} = 2500^{\circ}\text{K}$, $T = 1500^{\circ}\text{K}$, $\lambda = 1$ cm.

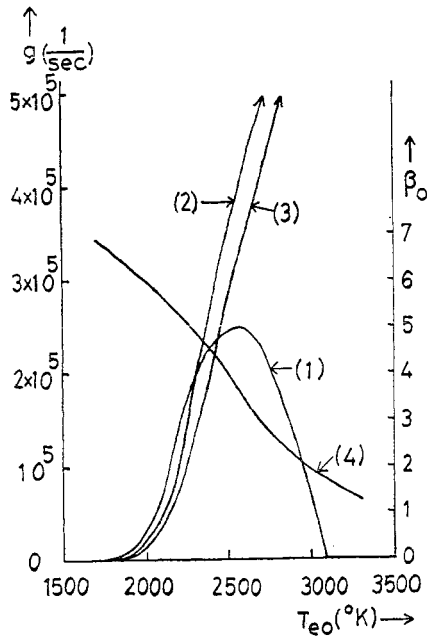


FIG. 12.—(A) Graph of growth rate vs. electron temperature (ionization mode). (1) $B = 5.0$ tesla; (2) $\beta_0 = 5.0$; (3) Magnetically induced elevated electron temperature ($\eta = 0.75$, $V = 10^8$ m/sec). For all three curves:— $T = 1500^{\circ}\text{K}$, $\alpha = \pi/4$, $\lambda = 1$ cm. (B) Graph of Hall parameter vs. electron temperature. (4) $B = 5.0$ tesla (right hand scale).

and at higher temperatures, above approximately 3000°K, the waves are damped.

The reason for the decrease of g towards lower temperatures is partly due to the decreasing value of $T_{e0} - T$. Since $j_0^2/\sigma_0 \propto (T_{e0} - T)$ and $(j^2/\sigma)' \propto j_0^2/\sigma_0$, decreasing $T_{e0} - T$ means decreasing $(j^2/\sigma)'$ and therefore the growth rate falls off. However if we were to decrease T keeping $T_{e0} - T$ constant g will still decrease with decreasing T_{e0} . (see Fig. 13 curve 1). This is due to the decrease in the ionization and recombination rates at lower temperatures. The growth rate is limited here by the rate at which the seed can ionize. This can be seen by comparing curves 1 and 2 in Fig. 13. In curve

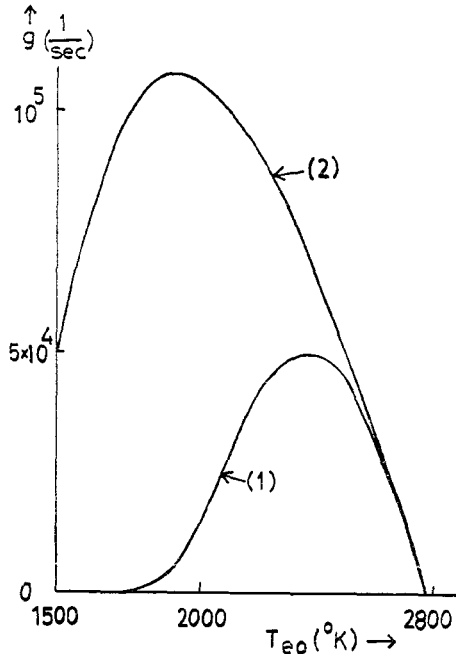


FIG. 13.—Graph of growth rate vs. electron temperature with constant (ionization mode). (1) $b = 1.1 \times 10^{-20}$; (2) $b = 10^{-15}$. For both curves:— $T_{e0} - T = 300^{\circ}\text{K}$, $\alpha = \pi/4$, $\lambda = 1$ cm, $B = 5.0$ tesla.

2 we have arbitrarily multiplied the ionization and recombination coefficient by a factor 10^5 . The growth rate does not decrease in curve 2 till 1800°K; we conclude therefore that the infinite ionization and recombination rate approximation overestimates the growth rate for temperatures below 2500°K but gives a good approximation for temperatures above 2500°K.

The growth rate, g , decreases as T_{e0} increases past 2500°K in Fig. 12 curve 1 not because of the increasing degree of ionization, but because β_0 decreases at fixed B due to ν_0 increasing with temperature. This can be seen from curves 2 and 4 on Fig. 12: curve 4 is β_0 vs. T_{e0} and $\beta_0 \sim 1$ when the wave becomes stable; curve 2 shows g vs. T_{e0} with $\beta = 5$, i.e. B increasing with T_{e0} , and here g shows no maximum with T_{e0} in the plotted range. For $\beta = 5$ the growth rate does not start to fall off due to the large degree of ionization until $T_{e0} \approx 5000^{\circ}\text{K}$ (see Fig. 14 curve 1). At temperatures above 5000°K the value of α for maximum g (α_{max}) shifts towards $\pi/2$. This is due to the decreasing value of ρ and therefore the Ohmic heating becomes dominated by the T_e^* terms and the approximate $\sin 2\alpha$ dependence of the growth rate (see Section 5(g)) changes to $\sin^2 \alpha$.

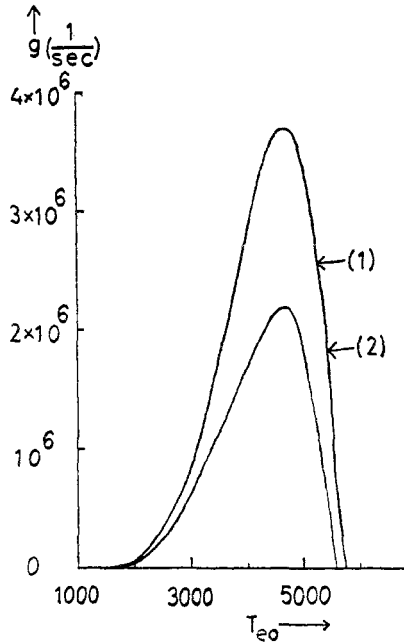


FIG. 14.—Growth rate vs. electron temperature (ionization mode). (1) $\beta_0 = 5.0$;
 (2) Magnetically induced elevated electron temperature ($\eta = 0.75$, $V = 10^8$ m/sec).
 For both curves:— $T = 1500^\circ\text{K}$, $\lambda = 1$ cm, $\alpha = \pi/4$.

If instead we increase T_{e0} by increasing B to produce more magnetically induced nonequilibrium ionization with fixed load factor in an ideal Faraday mode generator, where $j_0 = \sigma_0 V B (1 - \eta)$, then g as a function of T_{e0} is shown in Fig. 12 curve 3. The growth rate increases monotonically for the values of T_{e0} plotted. This is because, for fixed load factor $\eta (= r_L/r_L + r_P)$ the value of B required to produce an electron temperature T_{e0} in the steady state is given by

$$\sigma_0 V^2 B^2 (1 - \eta)^2 = 3n_{e0} k (T_{e0} - T) \left[v_{\text{coll}0} \frac{m_e}{m_s} + v_{BO} \frac{m_e}{m_n} \right]$$

$$\therefore \beta_0 = \frac{e}{m_e v_0} \left[\frac{3n_{e0} k (T_{e0} - T)}{\sigma_0 V^2 (1 - \eta)^2} \left\{ v_{\text{coll}0} \frac{m_e}{m_s} + v_{BO} \left(\frac{m_e}{m_n} - \frac{m_e}{m_s} \right) \right\} \right]^{1/2}$$

for $m_n < m_s$ the temperature dependence of β_0 can be seen from

$$\beta_0 > \left[\frac{3k(T_{e0} - T)}{m_s v^2 (1 - \eta^2)} \right]^{1/2}$$

Therefore β_0 increases with temperature and the growth rate increases with it. However at higher temperatures the finite degree of ionization limits the wave and the growth rate falls to zero (see Fig. 14 curve 2).

Close comparison of these results with experiment is not yet possible. This is because experiments to date observe the existence of fluctuations in electron density in the plasma but do not determine the growth rate of these fluctuations. It is possible of course that the dependence of the growth rate on the electron temperature could be inferred from the fluctuation amplitude at a fixed point in the plasma for various

temperatures. However this assumes two things; firstly that the initial perturbation is independent of the electron temperature, or varies with it in some known way; and secondly that the fluctuations do not reach some steady non-linear amplitude before reaching the point of observation.

(f) *Dependence of the instability on K*

Figure 2 shows the dependence of the real part of ω_r on K for $\alpha = \pi/4$, $T_{e0} = 2500^\circ\text{K}$, and $B = 5.0$ tesla. The dispersion curve is a straight line through the

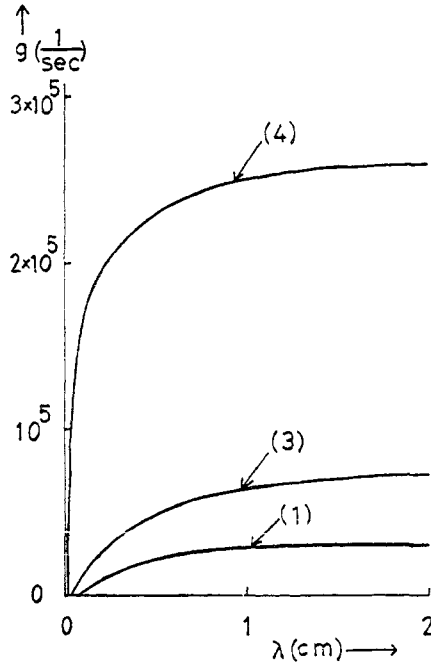


FIG. 15.—Growth rate vs. wavelength (ionization mode). (1) $T_{e0} = 2000^\circ\text{K}$; (2) $T_{e0} = 2500^\circ\text{K}$; (3) $T_{e0} = 3000^\circ\text{K}$. For all curves:— $T = 1500^\circ\text{K}$, $\alpha = \pi/4$, $B = 5.0$ tesla.

origin therefore both the phase velocity (ω_r/K) and the group velocity ($d\omega_r/dK$) are independent of K .

The imaginary part of $\omega(g = -\omega_I)$, however, varies with K , and we see from Fig. 15 that, for various temperatures, the growth rate decreases, as expected, when λ , the wavelength, decreases. This is due mainly to the thermal conduction losses which vary as $1/\lambda^2$, and also to a lesser degree to the radiation term which varies as $1/\sqrt{\lambda}$.

We note that the elevated electron temperature steady state is unstable for infinite wavelength. However, we have imposed no finite length boundary conditions on the electron temperature, and more important on \mathbf{j}' , and so in practice a characteristic length of the system would place a limit on the wavelength.

(g) *Physical nature of the waves*

The development of a physical picture of the waves, how they move and how they grow, is of considerable interest; but the interplay of the physical mechanisms in the wave is obscured by the number and complexity of the terms, especially in the

energy equation. However, if we assume that n_e^* and T_e^* are sinusoidal in space then we can describe briefly the way in which the electrons move in the fluctuations and the mechanism by which the fluctuations themselves move.

In any sinusoidal fluctuation n_e^* it follows from the zero longitudinal component of the current ($\nabla \cdot \mathbf{j}' = 0$) that the fluctuation in the magnitude of the longitudinal electron drift velocity is given by $|v_e|' = -n_e^*$. Therefore the electrons stream through the fluctuation with decreased velocity in the peaks of n_e^* and increased velocity in the troughs of n_e^* . The fluctuation itself does not tend to convect with the electrons since the assumption that $n_i = n_e$ would require the ions to move with the wave which is incompatible with our assumption of stationary ions.

The mechanism of movement of the waves is, in fact, an inequality of the heating in the different slopes of a sinusoidal wave. The terms contributing to this are of course the gradient terms in equation (3), the energy equation. The other terms are in phase with either n_e^* or T_e^* , which, we have seen, usually have a phase difference either of nearly zero (I.M.) or of nearly π (F.T.M.), and contribute only to the growth or decay of the wave.

When equation (3) is linearised we obtain two gradient terms, viz. $-3/2 k j_{0w}/e \partial T_e'/\partial y$, i.e. convection of hot electrons, and $k T_{e0} j_{0w}/n_{e0} e \partial n_e'/\partial y$, i.e. compressional heating.

For the Ionization Mode in most of the temperature regime investigated here, $n_e^* \gg T_e^*$; therefore compressional heating is the dominant effect. The electrons are heated as they stream into the peaks of n_e^* , which correspond almost exactly to the peaks of T_e^* , and cooled as they leave the peaks of n_e^* ; therefore the sinusoidal wave has an inequality in $\partial T_e^*/\partial t$ which causes the wave to move in a direction opposite to that of the steady state electron drift.

However, at higher temperatures where $\partial \log n_e/\partial \log T_e \rightarrow 0$, we can have the situation in the ionization mode where $T_e^* \gg n_e^*$, and the convection of hot electrons dominates. The direction of the wave movement is reversed since the convection heats the electrons where they are leaving the peaks and cools them where they are entering the peaks. The reversal of the phase velocity should occur when the effect of compressional heating and the convection of hot electrons are equal in magnitude. This occurs when $\partial \log n_e/\partial \log T_e = 3/2$, i.e. when $T_{e0} = 4650^\circ\text{K}$ for $n_s = 10^{22} \text{ 1/m}^3$. Comparison with Fig. 18 shows this to be the correct temperature for the reversal of the phase velocity.

The phase velocity is also zero when $\alpha = \pm\pi/2$, since then both gradient terms are zero (see Fig. 8).

Physically the source of the instability is the enhanced Ohmic heating in the peaks of n_e^* and T_e^* . However, without a magnetic field, the perturbations of the elastic loss to the heavy particles is greater than the perturbation of the Ohmic heating, and the wave is damped. The effect of a magnetic field is to increase the fluctuations in the current, and hence the Ohmic heating, for a given n_e^* and T_e^* , until, for $\beta_0 \sim 1$, the perturbed Ohmic heating becomes larger than the sum of perturbed elastic and other losses, and therefore the wave grows.

The extra components of \mathbf{j}' due to the magnetic field come from $\mathbf{F}' \times \mathbf{B}$ drift currents and the fluctuations of the hall parameter. The linearisation of the Ohm's law gives, $j'_x = j_0[\sigma^* \sin \alpha + (\sigma^* - \beta^*)\beta_0 \cos \alpha]$. Therefore for $\beta_0 \gg \beta_{\text{crit}}$ we can write $j'_x \approx j_0(\sigma^* - \beta^*)\beta_0 \cos \alpha$.

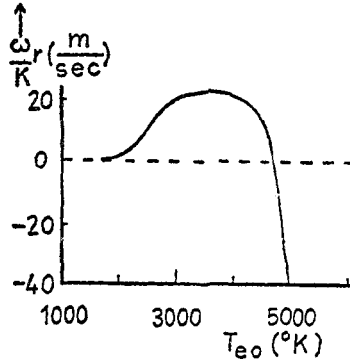


FIG. 16.—Graph of phase velocity vs. electron temperature (ionization mode). $T = 1500^\circ\text{K}$, $\lambda = 1\text{ cm}$, $\alpha = \pi/4$, $B = 5.0\text{ tesla}$.

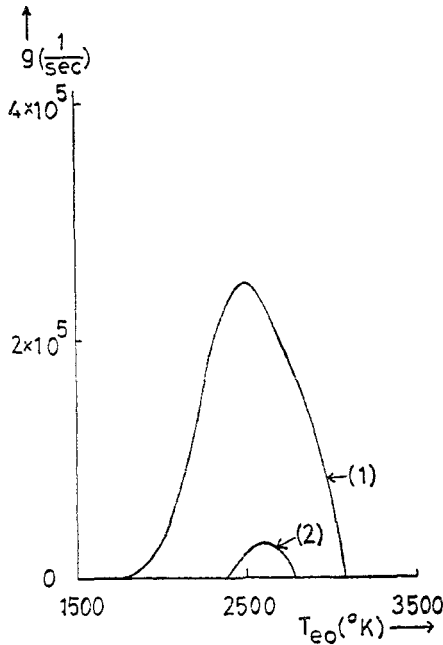


FIG. 17.—Graph of growth rate vs. electron temperature (ionization mode). (1) with normal radiation term for the caesium resonance lines; (2) with radiation term = 10 times caesium radiation. For both curves $T = 1500^\circ\text{K}$, $\alpha = \pi/4$, $B = 5.0\text{ tesla}$, $\lambda = 1\text{ cm}$.

Now the perturbation of the Ohmic heating is given by

$$\begin{aligned} \left(\frac{j^2}{\sigma}\right)' &= \frac{2\mathbf{j}_0 \cdot \mathbf{j}'}{\sigma_0} - \frac{j_0^2}{\sigma_0} \sigma^* \\ &= \frac{2j_0 j_x' \sin \alpha}{\sigma_0} - \frac{j_0^2}{\sigma_0} \sigma^*. \end{aligned}$$

The positive part of this is of course the source of the instability and substituting for j_x' give a source term $\propto \sin 2\alpha$, i.e. we expect the growth rate to maximise at $\alpha = \pi/4, 5\pi/4$ which is in accordance with the results of the calculations. The reason for this, then, is that magnetically induced components of j_x' maximise at $\alpha = 0$,

while, for a given j_x' , the Ohmic heating maximises at $\alpha = \pi/2$, so the maximum of the growth rate is a compromise between the two. Also at lower values of β_0 where the ionization is damped the $\sin \alpha$ term of j_x' begins to dominate and the maximum of the growth rate, although it is negative, tends towards $\alpha = \pi/2$ (see Fig. 5).

(h) *Radiation transfer*

The foregoing results in general confirm the well known fact that the growth rate decreases with decreasing β_0 and for $\beta_0 < \beta_{0\text{CRIT}}$ the fluctuations are damped.

The undesirable effects of the instability could then be avoided by choosing experimental conditions such that $\beta_0 < \beta_{0\text{CRIT}}$. In the case of an MHD generator, since the power density is proportional to B^2 , then the higher the magnetic field the higher will be the output. Imposing the condition $\beta_0 < \beta_{0\text{CRIT}}$ is therefore an unsatisfactory way of avoiding fluctuations. We must therefore consider ways of damping the waves other than keeping β_0 as low as possible, which corresponds to keeping the perturbed Ohmic heating in the wave less than the losses. One method of doing this would be to try and increase the radiative energy transfer to cancel the Ohmic heating. The effect of arbitrarily increasing the radiation term for the caesium resonance lines by a factor of 10 is shown in Fig. 17. Curve (1) is g plotted against T_{e0} using the normal radiation term and curve (2) is g plotted against T_{e0} with the arbitrarily enhanced radiation. We conclude that if we can increase the radiation by an order of magnitude a substantial damping effect will be produced. Let us consider the radiation term in more detail. For the i th line the perturbation of the radiation transfer is exactly given by

$$R_i' = \left\{ \frac{3k^2 T_{e0}}{2hc} \sqrt{\frac{K n_{aG} \Delta \nu_i g_{Ei}}{\tau_i g_0}} \right\} \times \left(\frac{h\nu_i}{kT_{e0}} \right)^3 \frac{\exp\left(+\frac{h\nu_i}{kT_{e0}}\right)}{\left(\exp\left(\frac{h\nu_i}{kT_{e0}}\right) - 1\right)^2} T_e'$$

where

$$n_{aG} = n_a / \left(1 + \sum_j \exp\left(-\frac{h\nu_j}{kT_{e0}}\right) \right)$$

$$\therefore R_i' \propto \frac{\left(\frac{h\nu_i}{kT_{e0}}\right)^3 \exp\left(+\frac{h\nu_i}{kT_{e0}}\right)}{\left(\exp\left(\frac{h\nu_i}{kT_{e0}}\right) - 1\right)^2 \sqrt{1 + \sum_j \exp\left(-\frac{h\nu_j}{kT_{e0}}\right)}}$$

Assuming $\nu_1 = \nu_2$, R.H.S. maximises at $h\nu_1/kT_e \approx 2.7$, and the maximum value ≈ 1.0 . At $T_{e0} = 2000^\circ\text{K}$ $h\nu_1/kT_{e0} \approx 8.5$ for the caesium doublet and the R.H.S. has a value ≈ 0.1 . The radiation would be increased by a factor of 10 therefore if we could 'dope' the plasma up to the seed density with an element whose resonance line corresponds to $h\nu_1/kT_{e0} = 2.7$. (Note that the values of τ_i , $\Delta \nu_i$, and g_{Ei} do not change a great deal for atomic levels and they appear under a square root sign. Therefore maximising the radiation w.r.t. $h\nu_1/kT_{e0}$ is equivalent to maximising it with respect to the identity of the radiating element). However the wavelength corresponding to this value of $h\nu_1/kT_{e0}$ at 2000°K is $\sim 20,000 \text{ \AA}$, i.e. in the infrared; and resonance lines have much shorter wavelengths than this. It is unlikely therefore that the radiation can be substantially increased by optimising ν_1 .

Alternatively we could attempt to increase the radiation by increasing the number of radiating atoms. However, this may have undesirable chemical effects as well as increasing the internal plasma impedance by inelastic collisions; therefore the doping of the plasma may have to be kept to a minimum. If we increase the caesium density by a factor N say then the radiation increases by only a factor \sqrt{N} . This is because the absorption is increased as well as the emission being increased; also the electron density will be increased by a factor N , which, in the lower temperatures where coulomb collisions are not so important, will increase the Ohmic heating by a factor of N , while the radiation damping increases by only a factor of \sqrt{N} . However if, say, we add $N - 1$ other elements, all distinct, with doublet resonance lines that have ν_i of the order of that for caesium, but which do not overlap even after collision broadening, then the radiation will be increased by a factor of N if the density of each new element equals the caesium density. And if the ionization potential of these new elements is high enough they will not significantly alter the electron density. That is by increasing the total dope density by a factor N we this time obtain N times the radiation transfer compared with \sqrt{N} before. Mathematically this is because in the case of added dopes the radiation term is the sum of that of all the different components, whereas in the first case the new radiation term is obtained by substituting the new caesium density into the term under a square root sign. Physically the greater increase in radiation transfer in the case with added dopes is due to the fact that the absorption for each wavelength has approximately the value for the caesium doublet which is unchanged, while the total energy emitted is increased.

The object of removing the fluctuations of the electron density in an MHD generator is to reduce the effective plasma impedance. It may be that the plasma impedance can be minimized at an optimum dope density, where the radiation transfer decreases the fluctuation amplitude while at the same time the increase in the damaging effects of radiation escape and inelastic scattering is not too large.

(i) *Growth rates in different gas mixtures*

The growth rate of the ionization mode was calculated as a function of temperature for mixtures of argon and potassium, helium and caesium, and helium and potassium, as well as argon and caesium previously considered in detail. The results are shown in Fig. 18. We see that for fixed magnetic field the general form of all the curves is the same. The differences in g between the different gas mixtures are due to the differences in the Hall parameter, the electron-heavy particle thermal coupling, the radiative transfer, the thermal conduction and the relative importance of coulomb and neutral collisions. A detailed description of all the differences would be rather complicated, however a brief discussion of the four main differences will be given here.

First of all, for a given seed, helium as the neutral gas always leads to more unstable waves than argon at fixed electron and gas temperatures. Due to the higher cross section for momentum transfer in Helium the value of β_0 is lower and this tends to damp the wave. However the decrease in β_0 is accompanied by an increase in the Ohmic heating required to produce a given value of $T_{e0} - T$ in the lighter helium, since the thermal coupling between the neutrals and the electrons is proportional to m_e/m_n . Therefore, because the amplifying term in the energy equation is proportional to $j_0^2/\sigma_0 \times \beta_0$ (see equation (9)) and the increase in j_0^2/σ exceeds the decrease

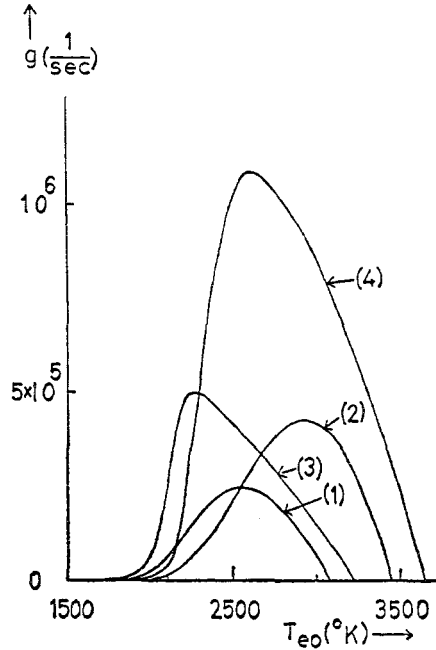


FIG. 18.—Graph of growth rate vs. electron temperature for various gas mixtures (ionization mode). (1) Argon and caesium; (2) argon and potassium; (3) helium and caesium; (4) helium and potassium. For all curves:— $T = 1500^\circ\text{K}$, $\lambda = 1\text{ cm}$, $\alpha = \pi/4$, $B = 5.0\text{ tesla}$, and the seed fraction = 0.001.

in β_0 , the growth rate for helium is higher than for argon at the same electron and gas temperatures.

Secondly, for a given neutral gas, potassium has a larger maximum of growth rate than caesium. This is similar to the first point since it is due to the fact that, when coulomb collisions are important, higher Ohmic heating is required in potassium to produce a given difference in the gas and electron temperatures than in caesium. Although potassium and caesium have different ionization potentials the peaks of g occur at different temperatures, where n_e is approximately equal for both gases, therefore β_0 is constant. The reason for the increase j_0^2/σ_0 is then due to the smaller mass of the potassium compared with caesium, since the elastic loss to the ions is proportional to m_e/m_i . But we see that at low temperatures the growth rate for caesium can exceed that for potassium and this brings us to the third point, viz. the maximum of g for potassium is shifted towards higher temperatures compared to that for caesium. The reason for this is simply the higher ionization potential of potassium compared to caesium which gives a lower electron density for a given electron temperature. At lower temperatures the growth is limited by the finite ionization and recombination rates and, since these are proportional to n_{e0}^2 their damping effect is greater in potassium than in caesium; also at low temperatures neutral collisions tend to dominate and the elastic losses are proportional to n_{e0} , therefore, for a given $T_{e0} - T$, j_0^2/σ_0 is smaller in potassium than in caesium, while β_0 is practically unchanged. The combination of these effects gives a lower growth rate for potassium compared with caesium in the same neutral gas at low temperatures. At high temperatures the ionization and recombination rates cease to be limiting, and the

increasing importance of coulomb collisions causes the difference in the electron-heavy particle thermal coupling to decrease since potassium is lighter than caesium; also the Hall parameter is now larger for potassium than for caesium (due to the lower coulomb collision frequency) and this gives a larger g for potassium at high temperatures. Thus, for potassium, the maximum of g is shifted towards higher temperatures compared with that for caesium.

Fourthly, for a given seed, the maximum of g for helium is shifted towards lower temperatures compared to that of argon. The reason for this is that the cross-section for momentum transfer is higher for helium than for argon (for helium (OVCHARENKO, 1969) $q_{en} = 9.7 \times 10^{-20} \text{m}^2$), and the Hall parameter at a given temperature is therefore lower. This does not give us a lower growth rate for helium, since the thermal coupling effect due to the different masses dominates; however it does mean that the decrease in g due to decreasing Hall parameter at high temperatures starts at a lower temperature for helium than for argon. Hence the maximum of g is shifted to lower temperatures.

6. SUMMARY

The analysis of the dispersion relation for electrothermal waves show that there are two modes of oscillation, viz. the fast thermal mode, and the ionization mode. The fast thermal waves are always damped, while the ionization waves are unstable under certain plasma conditions, with maximum growth rates typically between 10^5 and 10^6 . This is the previously reported ionization instability and it is a damaging instability as far as MHD generators are concerned in that the plasma typically spends 10^{-3} sec in the generator section; therefore a small disturbance in electron density could be amplified by a factor of over 100.

The calculated dependence of the growth rate on α , β_0 and K is in agreement with the most recent experimental and theoretical papers. As far as the dependence on T_{e0} is concerned the damping effect of finite ionization and recombination rates at temperatures below 2500°K has been demonstrated, while at higher temperatures the damping effect of the degree of ionization approaching 1 has been shown not to be significant for caesium until temperatures above 5000°K . However for fixed magnetic field the growth rate decreases rapidly with increasing electron temperature above 2500°K , due to decreasing β_0 as Coulomb collisions become important, and the wave is damped at temperatures above approximately 3000°K , (these temperatures depend only weakly on the magnitude of B).

If the radiation transfer in the plasma could be increased by an order of magnitude the wave could be stabilized, or at least the growth rate could be substantially reduced. Obtaining such an increase however may not be possible without radically changing the plasma parameters.

The frequency of the ionization instability is low ($\sim 10^4$ c/s at $\rightarrow \lambda \sim 1$ cm) and it is only by virtue of its fast growth rate that we can justify neglecting perturbations of the neutral gas. At low growth rates ($\sim 10^4$ 1/sec say) this assumption must be untenable and sonic effects will have to be included. The sonic effects will probably be damping since the expansion of the gas provides a means by which energy can be dissipated in the electron density peaks. However this remains to be seen, and a unified low temperature MHD instability theory, combining the magnetosonic and electrothermal effects, is therefore necessary for the evaluation of low growth rates.

Acknowledgment—During the course of this work, A. H. NELSON was supported by a Science Research Council Grant.

REFERENCES

- ANGROLOV V., ASINOVSKI E., BATYENIN V., LOPATSKI G. and CHINNOV V. (1968) *Int. Symp. Magneto hydrodynamic Electrical Power Generation, Warsaw*. Paper SM-107/144.
- BATES D. R., KINGSTON A. E. and MCWHIRTER R. W. P. (1962a) *Proc. R. Soc.* **A267**, 297.
- BATES D. R., KINGSTON A. E. and MCWHIRTER R. W. P. (1962b) *Proc. R. Soc.* **A270**, 297.
- CORLISS C. H. and OZMAN W. R. (1962) *NBS monograph* 53.
- GRIEM H. R. (1964) *Plasma Spectroscopy*. McGraw-Hill, New York.
- HEYWOOD J. B. and WRIGHT J. K. (1967) *Phil. Trans. R. Soc.* **A261**.
- HINNOV E. and HIRSCHBERG J. G. (1962) *Phys. Rev.* **125**, 795.
- KERREBROCK J. (1964) *AIAA J.* **2**, 6.
- LO SURDO C. (1967) *Nuovo Cim.* **52B**, 429–454.
- LOUIS J. F. (1968) *Int. Symp. Magnetohydrodynamic Electrical Power Generation, Warsaw*. Paper SM-107/50.
- LUTZ M. A. (1967) *AIAA J.* **5**, 8.
- MCCUNE J. E. (1964) *Proc. Int. Symp. Magnetohydrodynamic Electrical Power Generation, Paris*. p. 523.
- NEDASPASOV A. (1966) Electricity from MHD. *Proc. Salzburg Symp.* Vol. 2, p. 345.
- OVCHARENKO V. (1969) to be published (present address, High Temperature Institute, Moscow).
- ROSA R. J. (1962) *Physics Fluids* **5**, 334.
- SHAW J. F., KRUGER C. H., MITCHNER M. and VIEGAS J. R. (1966) Electricity from MHD. *Proc. Salzburg Symp.* Vol. 2, p. 77.
- SHIPUK I. YA. and PASHKIN S. V. (1968) *Soviet Phys. Dokl.* **12**, 10.
- ZETTWOOG P. (1966) Electricity from MHD. *Proc. Salzburg Symp.* Vol. 2, p. 307.
- ZUKOSKI E. E. and GILPIN R. R. (1967) *Physics Fluids* **10**, 9.